JACS
JOURNAL OF THE AMERICAN CHEMICAL SOCIETY
Article
pubs.acs.org/JACS

Controlled Synthesis of Cell-Laden Microgels by Radical-Free Gelation in Droplet Microfluidics

Torsten Rossow,[†] John A. Heyman,[‡,§] Allen J. Ehrlicher,[‡,∥,⊥] Arne Langhoff,[○] David A. Weitz,[‡,#] Rainer Haag,[†] and Sebastian Seiffert*[,†,‡,▽]

[†]Freie Universität Berlin, Institute of Chemistry and Biochemistry, Takustr. 3, D-14195 Berlin, Germany
[‡]Harvard University, School of Engineering and Applied Sciences, 29 Oxford Street, Cambridge, Massachusetts 02138, United States
[§]HabSel, Inc., One Broadway, 14th Floor, Cambridge, Massachusetts 02142, United States
[∥]Translational Medicine Division, Brigham and Women's Hospital, Boston, Massachusetts 02115, United States
[⊥]Harvard Medical School, Boston, Massachusetts 02115, United States
[○]Clausthal University of Technology, Institute of Physical Chemistry, Arnold-Sommerfeld-Str. 4, D-38678 Clausthal-Zellerfeld, Germany
[#]Harvard University, Department of Physics and Kavli Institute for Bionano Science and Technology, 29 Oxford Street, Cambridge, Massachusetts 02138, United States
[▽]Helmholtz-Zentrum Berlin, F-I2 Soft Matter and Functional Materials, Hahn-Meitner-Platz 1, D-14109 Berlin, Germany

Supporting Information

ABSTRACT: Micrometer-sized hydrogel particles that contain living cells can be fabricated with exquisite control through the use of droplet-based microfluidics and bioinert polymers such as polyethyleneglycol (PEG) and hyperbranched polyglycerol (hPG). However, in existing techniques, the microgel gelation is often achieved through harmful reactions with free radicals. This is detrimental for the viability of the encapsulated cells. To overcome this limitation, we present a technique that combines droplet microfluidic templating with bio-orthogonal thiol−ene click reactions to fabricate monodisperse, cell-laden microgel particles. The gelation of these microgels is achieved via the nucleophilic Michael addition of dithiolated PEG macro-cross-linkers to acrylated hPG building blocks and does not require any initiator. We systematically vary the microgel properties through the use of PEG linkers with different molecular weights along with different concentrations of macromonomers to investigate the influence of these parameters on the viability and proliferation of encapsulated yeast cells. We also demonstrate the encapsulation of mammalian cells including fibroblasts and lymphoblasts.

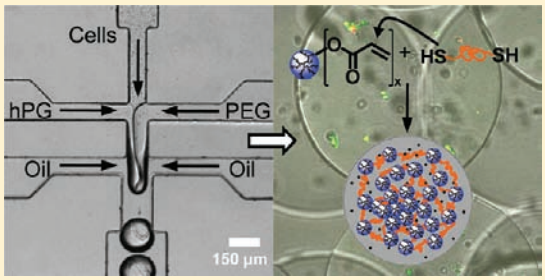

INTRODUCTION

Hydrogels are highly hydrated, cross-linked polymer networks which are valuable for many biological applications[1,2] such as those in drug delivery,[3−5] biosensing,[6] and tissue engineering.[7−11] In particular, hydrogels with micrometer-scale dimensions are useful as scaffolds for cell encapsulation, since they are injectable, can be manipulated with micropipets or microsyringes, and can be used as building blocks to create larger, uniformly built tissue.[12,13] Microgel matrixes also allow for a continuous supply of the embedded cells with smaller molecules such as nutrients, oxygen, metabolites, hormones, peptides, and small proteins.[14] Nevertheless, they can be transplanted without treatment with immune suppressing medicals, because bigger substances such as leucocytes, antibodies, and enzymes, which cause immune defense, are unable to penetrate the polymer matrix.[15] Moreover, microgels mimic the natural extracellular matrix and can be tailored to the cellular microenvironment. All these benefits make these particles attractive for applications in regenerative medicine. In addition, they are used as in vitro 3D-cell culturing systems, which are essential for drug testing due to differences in the behavior of cells on rigid 2D substrates and in 3D culture.[16,17]

For the fabrication of micrometer-sized hydrogel particles, droplet-based microfluidics is a powerful and versatile technique.[18−21] The concept of this approach is to use emulsion droplets as templates for the particle synthesis and to control the size, shape, and monodispersity of the microparticles by controlling the size, shape, and monodispersity of the premicrogel droplets. To achieve this, a stream of a premicrogel monomer solution (dispersed phase) is created in a microchannel, and its periodic break-up is induced by flow focusing with a second, immiscible fluid (continuous phase); this creates monodisperse, micrometer-sized droplets. After solidification, these droplets retain their uniform size and shape,

Received: January 15, 2012
Published: February 22, 2012

   dx.doi.org/10.1021/ja300460p | J. Am. Chem. Soc. 2012, 134, 4983−4989

yielding polymer particles with precisely controlled morphology.

Using this technique, several groups have developed microparticles for cell encapsulation. In many cases, these particles consist of natural polymers such as alginate.[22,23] However, natural polymers have several disadvantages: they differ in their composition from batch to batch since they are harvested from living organisms, the production of large volumes of natural polymers is limited, and they cannot be tailored to the specific cells to be encapsulated since their properties are determined by the species which produce them. By contrast, *synthetic* polymer matrixes can be prepared in large volumes, and their composition can be controlled as required for different cell lines.[24] This is achieved through the use of macromolecular precursors (macromonomers) which can be cross-linked through a polymer-analogous reaction. By this means, the properties of the polymer matrix can be determined by the polymer concentration, the precursor molecular weight and functionalization, and the chemistry of cross-linking.

Two popular types of synthetic, hydrophilic macromonomers that are highly biocompatible are hyperbranched polyglycerol (hPG) and polyethyleneglycol (PEG), both functionalized with methacrylate or acrylate groups. These macromonomers undergo rapid cross-linking upon exposure to UV light in the presence of photoinitiators,[25−28] which is a feature that has been employed extensively for the synthesis of macro-, micro-, and nanoscopic hydrogels: Hennink and colleagues used hPG macromonomers to prepare microgels by micromolding as well as photolithography and soft lithography in combination with free-radical photopolymerization.[29] Cell-laden microgel particles from photopolymerized PEG-macromonomers were also prepared by Doyle and co-workers using stop-flow lithography[30] and by Pishko and co-workers using photolithography.[31] Moreover, cell-laden microgels consisting of both hPG and PEG have been fabricated using droplet-based microfluidics.[32] With this approach, the microgel elasticity can be increased in comparison to pure hPG gels,[28,29] making these particles favorable for cell encapsulation.[33] Since photoinitiators and UV irradiation are potentially cytotoxic,[27,34] this recent work focused on the use of thermally generated radicals. However, despite the biocompatibility and favorable elasticity of the hPG−PEG polymer matrixes, the presence of free radicals during their formation is detrimental for cell viability.

The use of harmful radicals can be circumvented through the use of radical- and catalyst-free, bio-orthogonal click reactions. For example, the thiol−ene reaction of the Michael type can be used to cross-link hPG and PEG.[35−38] The bio-orthogonality of this reaction is comparable to that of the strain-promoted azide−alkyne cycloaddition, since it was shown to be selective versus biological amines.[39] It can only interfere with the rarely occurring amino acid cystein,[40] which, however, is also a problem of the strain-promoted azide−alkyne cycloaddition.[41] In addition, the thiol-Michael addition only requires substrate syntheses with a low number of steps that each have high yield, and the applicability of the thiol-Michael addition for in situ cell encapsulation has been demonstrated by Hubbell and co-workers[42] and Feijen and co-workers,[43] who proved it to be harmless to cells. Nevertheless, this chemistry has not to date been combined with droplet-microfluidic particle templating to produce monodisperse, cell-laden microgels.

In this paper, we use thiol−ene click chemistry in droplet microfluidics to fabricate monodisperse, cell-laden hPG−PEG microgels, as illustrated in Figure 1. The gelation of these microgels is achieved via the nucleophilic Michael addition of dithiolated PEG macro-cross-linkers to acrylated hPG building blocks and does not require any initiator. We systematically vary the gel properties through the use of PEG linkers with different molecular weights along with different concentrations of macromonomers to investigate the influence of these parameters on the viability and proliferation of yeast cells. We also demonstrate the encapsulation of mammalian cells.

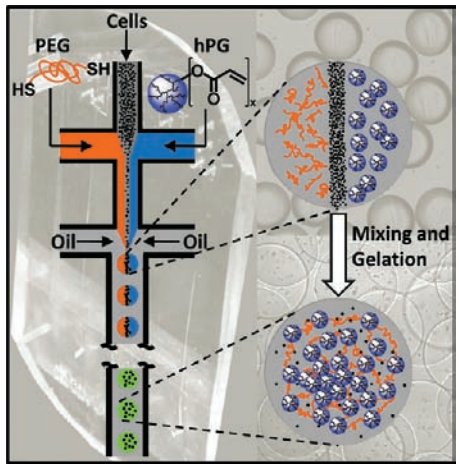

Figure 1. Microfluidic emulsification of aqueous solutions containing dithiolated PEG macro-cross-linkers, acrylated hPG building blocks, and cells. Subsequent mixing of the three liquids inside the monodisperse droplets leads to droplet gelation by thiol-Michael addition of the macromonomers, thereby forming micrometer-sized, cell-laden hydrogel particles.

RESULTS AND DISCUSSION

Fabrication of Cell-Laden Microgels. For the fabrication of cell-laden microgels, we proceed in a stepwise manner: first, we prepare two sets of aqueous precursor solutions, one containing hPGs with a weight-average molecular weight (M_w) of 16.5 kDa functionalized with 10 acrylate groups ($hPG_{16.5}Dea$), and the other containing PEG-diamines with different molecular weights. The PEG-diamines are then converted with 2-iminothiolane hydrochloride to yield thiol-terminated PEG (PEG-dithiol) in situ, as illustrated in Scheme 1. Then, both precursor solutions are injected into a microfluidic device, along with a solution that contains cells. By this means, premicrogel droplets are formed; these are subsequently gelled to yield cell-laden micogel particles.

During the conversion of PEG-diamine to PEG-dithiol, 2-iminothiolane hydrochloride is used in hypostoichiometric amounts (0.75 equiv per amine group) to reduce its potential cytotoxicity. The kinetics of this thiol formation was studied with $PEG_{1.5\ kDa}$ by Ellman's test:[44] The Ellman's reagent 5,5′-dithiobis(2-nitrobenzoic acid) reacts with thiols to form yellow-colored 2-nitro-5-thiobenzoate; the absorbance of this product at 412 nm can be tracked by UV−vis spectroscopy and serves as a measure of the relative concentration of thiols. This test shows that the simultaneous formation of free thiols and their elimination due to formation of disulfides results in a maximal thiol concentration after about 20 min, while a moderately high concentration of free thiols is present for a period of about 90 min, as shown in Figure 2. Performing the microfluidic experiment on this time scale therefore ensures that hydrogels form with reproducible properties.[45]

dx.doi.org/10.1021/ja300460p | J. Am. Chem. Soc. 2012, 134, 4983−4989

Scheme 1. Formation of Gel Particles by Cross-Linking of Hyperbranched Polyglycerol (hPG) and Polyethyleneglycol (PEG)

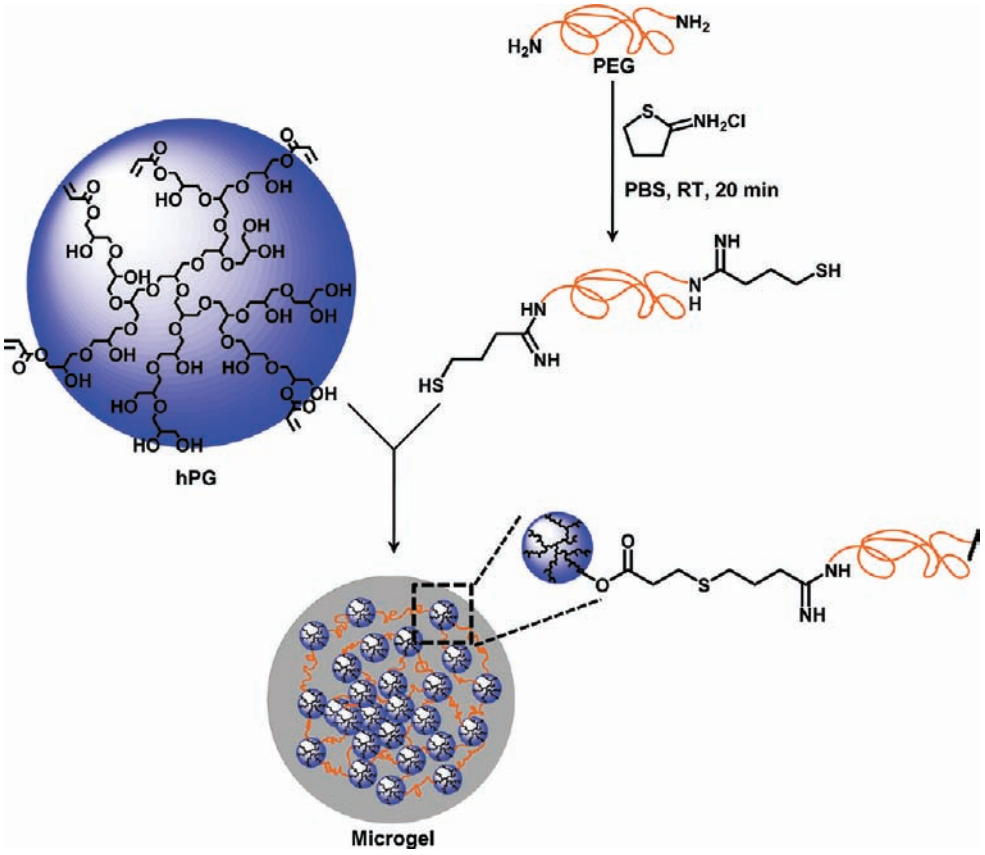

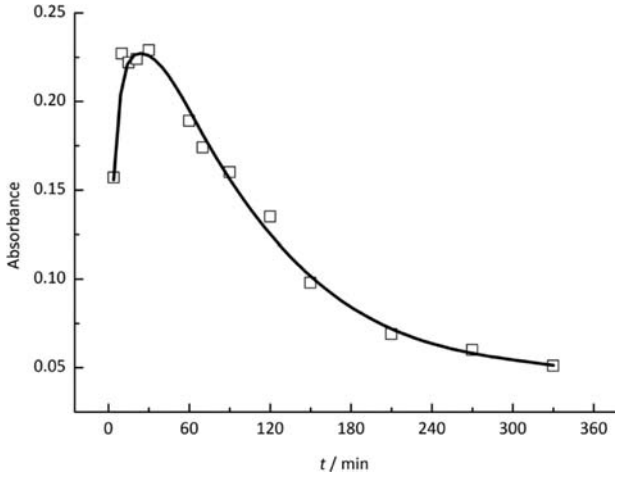

Figure 2. Kinetics of the conversion of PEG-diamine (1.5 kDa) with 1 equiv (per amine group) of 2-iminothiolane hydrochloride as determined by Ellman's test. Ellman's reagent 5,5′-dithiobis(2-nitrobenzoic acid) reacts with thiols and forms yellow-colored 2-nitro-5-thiobenzoate; the absorbance of this product at 412 nm is tracked with UV−vis spectroscopy and serves as a measure of the relative concentration of thiols. The line was drawn manually to guide the eye.

To create monodisperse premicrogel droplets as templates for the particle syntheses, we use poly(dimethylsiloxane) (PDMS) microchannels with two sequential cross-junctions fabricated by soft lithography,[46] as shown in Figure 3A. The two precursor solutions, $hPG_{16.5}Dea$ and PEG-dithiol, and the cell-containing medium are injected into three separate inlets of these devices, as shown in Figure 3B. After their injection, these three fluids meet at the first cross-junction, where they form a laminar coflowing stream in the microchannel. In the second junction, periodic break-up of this stream is induced by flow-focusing with a fourth fluid which is an immiscible paraffin oil; this produces uniform premicrogel droplets with sizes in the range of 150−200 μm, depending on the flow rates and the viscosities of the precursor solutions, as shown in Figure 3C. By mixing of the three liquids inside the droplets (Figure 3D), the precursors react in a thiol-Michael reaction (Scheme 1) and form cell-laden microgels within a few minutes. Typical water-swollen product particles with cells encapsulated inside are shown in Figure 3E.

Yeast Cell Encapsulation. To optimize the microgel properties for the encapsulation of yeast cells, we study the influence of the microgel elasticity on the viability of the encapsulated cells. The microgel elasticity is controlled by the molecular weight of the PEG-cross-linker and by the total precursor concentration.[47] We vary both parameters through the use of PEGs with molecular weights of 1.5, 6.0, and 20.0 kDa. In each case we fabricate gels with a low and high total precursor concentration, as summarized and detailed in Table 1. For all these samples, the ratio of hPG to PEG is determined such that about five PEG spacers are linked to one hPG building block.

For the $PEG_{1.5\ kDa}$ and $PEG_{6.0\ kDa}$ cross-linkers, the resultant microgels (Samples 1−4 in Table 1) are highly loaded with yeast cells which are distributed homogeneously throughout the particles, as shown in Figure 3E. By contrast, no homogeneous distribution of cells is obtained in the case of $PEG_{20.0\ kDa}$ (Sample 5 in Table 1). Instead, this polymer yields particles

dx.doi.org/10.1021/ja300460p | J. Am. Chem. Soc. 2012, 134, 4983−4989

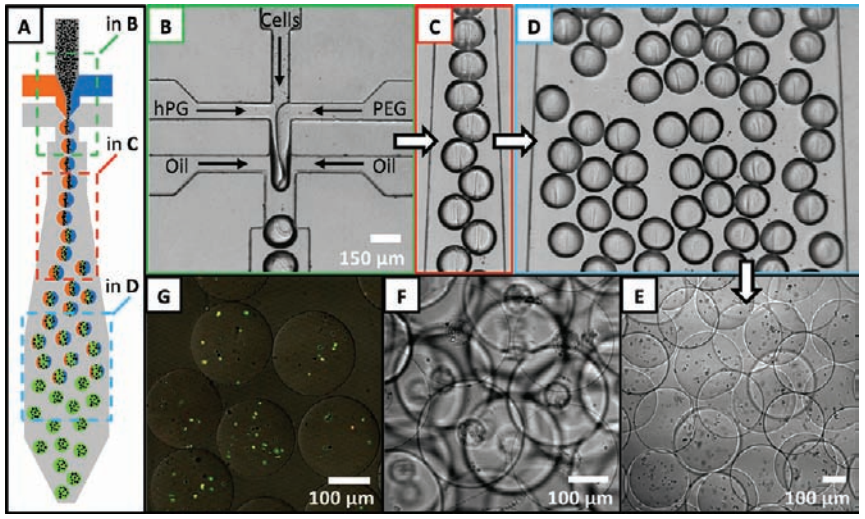

Figure 3. Droplet-microfluidic fabrication of yeast-cell-laden hPG–PEG microgel particles. (A) Schematic of the microfluidic device. (B) Two sequential cross-junctions serve to form monodisperse, micrometer-sized precursor droplets which consist of hPG, PEG, and cells. (C, D) Premicrogel emulsion obtained from the experiment in Panel B in the upper (C) and lower range (D) of a basin channel which is patterned right behind the two cross-junctions. (E) Micrograph of swollen, yeast-cell-laden microgel particles formed by gelation of the droplets in Panel D. (F) Core–shell-structured microgel Sample 5 (see Table 1 for details). (G) Viability of yeast cells encapsulated into hPG-$PEG_{6.0\,kDa}$ microgels with high precursor concentration (see Table 1 for details). Green staining denotes living cells, whereas orange or red staining marks dead cells.

Table 1. Compositions and Characteristics of Yeast-Cell-Laden hPG–PEG Microgel Particles

Sample	MW of PEG (kDa)	Concentration of hPG in Precursor Solution ($g \cdot L^{-1}$)	Concentration of PEG in Precursor Solution ($g \cdot L^{-1}$)	Degree of Microgel Swelling[a]	Viability of Encapsulated Yeast Cells (%)
1	1.5	500	156	39	93
2	1.5	1000	312	19	87
3	6.0	300	375	54	95
4	6.0	600	750	31	99
5[b]	20.0	200	833	/	/

[a]Calculated as $Q = (0.64w_{wet} - w_{dry})/w_{dry}$, with w_{wet} the wet and w_{dry} the dry weight of model microgels without any cell load. [b]Core–shell-type microgel morphology

with a core–shell-type morphology; the core contains all the cells, while the shell does not contain any cells, as shown in Figure 3F. We assume that the reason for this behavior is the high viscosity of the $PEG_{20.0\,kDa}$ solution, preventing efficient mixing of the cell phase with the precursor phases before gelation of the premicrogel droplets occurs. Since this particular microfluidic approach is not comparable to other microgels, it is not considered in the evaluation of the cell viabilities.

After the microfluidic experiments, the microgels are transferred from the oil phase into YPD (yeast extract, peptone, dextrose), a yeast cell culturing medium, where they swell to uniform sizes in the range of 250 to 350 μm depending on their composition. In YPD (pH 6.5), we do not observe any degradation of the microgels over time, whereas, for microgels dispersed in water, degradation through hydrolysis of the ester bond close to the thioether bond is observed over a time of several weeks.[48,49]

To investigate the viability of the encapsulated cells 90 min after their encapsulation, we perform a live–dead assay by adding two fluorescent dyes: Syto 9 is a green fluorescent dye that stains both living and dead cells, whereas propidium iodide is a red fluorescent dye that stains dead cells only. As a result, dead cells appear red or orange, whereas living cells appear green when observed with a fluorescence microscope. To relate the viabilities of the cells inside the microgels to the microgel composition and elasticity, we determine the degree of swelling of the microgel particles. This is done using model microgels with the same composition as the actual microgels, but without any cell load. After producing and washing these model microgels, we store them in an aqueous phase for a period of several hours to achieve equilibrium swelling. The concentration of the swollen microgel particles is then increased by centrifugation at 600 RCF for 10 min. Upon removal of the supernatant swelling agent with a pipet, the remaining particle suspension can be considered as a random close packing of spheres with a space filling of 64%. The degree of microgel swelling, Q, can then be determined gravimetrically by comparing the wet and dry weight of the concentrated particle suspension, w_{wet} and w_{dry}; we calculate it as $Q = (0.64w_{wet} - w_{dry})/w_{dry}$.

No distinct correlation is observed between the degree of microgel swelling, which is a measure of the microgel elasticity, and the cell viability, as demonstrated in Figure 4. The highest ratio of cell viability (~99%) is obtained with the $PEG_{6.0\,kDa}$ gels with high precursor concentration (Sample 4 in Table 1), as substantiated in Figure 3G. The degree of swelling of these particles lies between those of the low- and high-concentrated $PEG_{1.5\,kDa}$ gel matrixes, in which yeast cells have a viability of

dx.doi.org/10.1021/ja300460p | J. Am. Chem. Soc. 2012, 134, 4983–4989

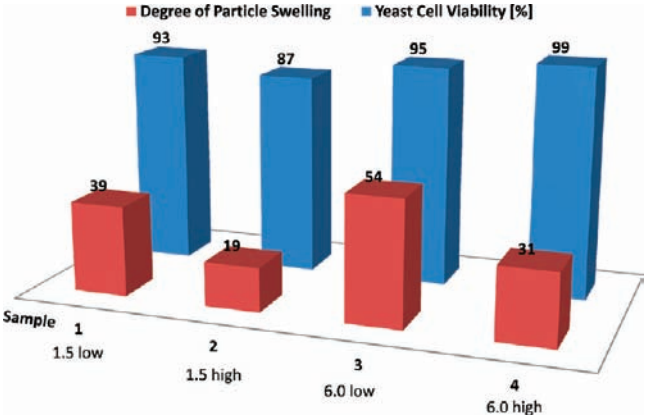

Figure 4. Degree of microgel swelling (red) and percentage viability of encapsulated yeast cells (blue) in hPG–PEG microgel particles with different compositions. The numbers 1.5 and 6.0 denote the molecular weights of PEG in kDa; the adjectives "low" and "high" signify the total precursor concentrations, as detailed in Table 1. The degree of swelling is calculated as $Q = (0.64w_{wet} - w_{dry})/w_{dry}$, with w_{wet} the wet and w_{dry} the dry weight of model microgels without any cell load.

93% and 87%. Hence, we assume that not only the macroscopic gel stiffness but also the nanoscale obstruction of the diffusion of nutrients and metabolites, which arises due to the presence of the polymer matrix, is an important factor for the cell viability. On the basis of our results and in agreement with the work of Bashir et al.,[26] this obstruction seems to be more pronounced in the $PEG_{1.5\ kDa}$ microgels than in the $PEG_{6.0\ kDa}$ microgels.

To substantiate this hypothesis, we use fluorescence correlation spectroscopy to monitor the diffusive motion of a low molecular weight dye, rhodamine 6G, which mimics the behavior of low molecular weight metabolites, inside the microgel particles. The presence of the polymer gel hinders the mobility of this dye; as a result, the diffusive motion of the dye is slowed. Moreover, its mean square displacement is no longer proportional to time; instead, the mean square displacement is proportional to time with an exponent $\alpha < 1$.[50,51] To account for this anomalous, subdiffusive behavior, we use an equation with the additional stretching exponent α to fit the fluorescence autocorrelation data.[52,53] With this procedure, we quantify the diffusive correlation time of the pure dye in water as $\tau_D = 0.3$ ms, along with an exponent $\alpha = 1$, which denotes normal Brownian diffusion. In the presence of the $PEG_{6.0\ kDa}$ gel matrix at high precursor concentration (Sample 4 in Table 1; 99% cell viability), the mobility of the dye decreases, exhibiting a correlation time of $\tau_D = 1.0$ ms and an exponent $\alpha = 0.83$, which denotes subdiffusive behavior. If the dye mobility is probed inside the highly concentrated $PEG_{1.5\ kDa}$ gel matrix (Sample 2 in Table 1; 87% cell viability), further deceleration is observed, leading to $\tau_D = 2.5$ ms and $\alpha = 0.83$. The exponent α can be considered as a measure of the obstacle concentration;[50] this concentration is the same for Samples 2 and 4, since their total precursor concentrations are similar. The correlation time τ_D depends on the obstacle size,[50] which can be associated with the cross-link density and distribution of mesh sizes in the polymer network. Our results for τ_D show that the $PEG_{1.5\ kDa}$ matrix imparts a more significant hindrance to the diffusivity of low molecular weight substances than does the $PEG_{6.0\ kDa}$ gel matrix, therefore obstructing the metabolism of encapsulated cells more profoundly. This result is in agreement with the lower cell viability in the $PEG_{1.5\ kDa}$ matrix compared to the cell viability in the $PEG_{6.0\ kDa}$ matrix.

To characterize the behavior of the yeast cells in the most favorable polymer matrix $PEG_{6.0\ kDa}$ in greater detail, these cells were observed overnight by microscopy, as shown in Figure 5A–E. This long-term observation shows that the cells proliferate in these microgels, despite their entrapment in a polymer gel which exhibits an elastic modulus in the range of a

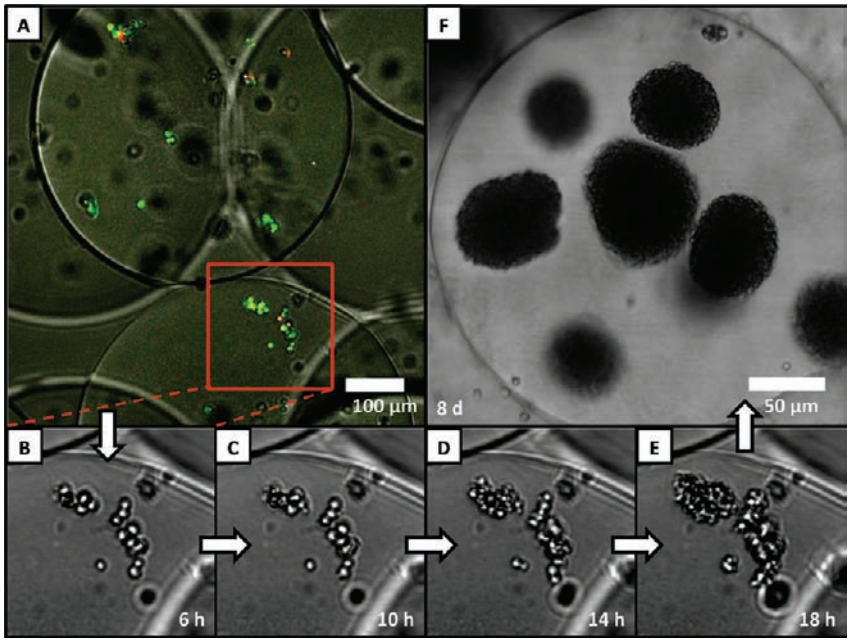

Figure 5. Viability of yeast cells encapsulated into hPG–PEG microgels. The samples were stained with Syto 9 (green dye, staining both living and dead cells) and propidium iodide (red dye, staining dead cells only) and then observed by bright field and confocal fluorescence microscopy. Green staining denotes living cells, whereas red or orange staining marks dead cells. (A–F) Yeast cells encapsulated into hPG–PEG microgels after (A) 2 h (B) 6 h, (C) 10 h, (D) 14 h, (E) 18 h, and (F) 8 days of storage after the microfluidic particle production.

dx.doi.org/10.1021/ja300460p | J. Am. Chem. Soc. 2012, 134, 4983–4989

few kilopascals, as determined by oscillatory shear rheology on a macroscopic gel sample with the same composition. Since no particle deformation is observed upon cell growth, the yeast cells apparently degrade the hydrogel in their environment. Even after 8 days, cells encapsulated in $PEG_{6.0\ kDa}$ microgels (Sample 4 in Table 1) are still alive and are able to proliferate extensively, forming huge colonies of cells, as shown in Figure 5F.

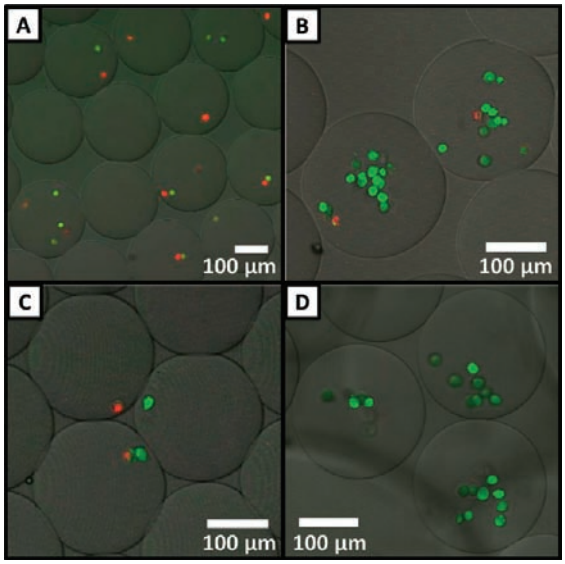

Figure 6. Viability of mammalian cells encapsulated into hPG–PEG microgels. Green staining denotes living cells, whereas red staining marks dead cells. (A) Lymphoblasts at low density. (B) Lymphoblasts at high density. (C) Fibroblasts at low density. (D) Fibroblasts at high density.

Mammalian Cell Encapsulation. To investigate the utility of the hPG–PEG microgels to encapsulate more complex mammalian cells, we use fibroblasts and lymphoblasts. The viability of these cells is again characterized by live–dead assays, staining living cells green and dead cells red (Figure 6). For both types of cells, the encapsulation experiments are performed at two different cell densities by varying the concentration of the cell-containing medium, as detailed in Table 2.

Table 2. Characteristics of Mammalian-Cell-Laden hPG–PEG Microgel Particles[a]

Cell Type	Cell Density	Number of Cells per Particle (Integer)	Cell Viability (%)
Lymphoblast	low	1 ± 1	52
Lymphoblast	high	8 ± 4	76
Fibroblast	low	2 ± 1	59
Fibroblast	high	7 ± 4	89

[a]The microgel matrix was prepared from a 600 $g{\cdot}L^{-1}$ $hPG_{16.5}Dea$ and a 750 $g{\cdot}L^{-1}$ $PEG_{6.0\ kDa}$ precursor solution.

For lymphoblasts at a low cell density, a viabilitiy of about 52% is retained upon encapsulation into a $PEG_{6.0\ kDa}$ matrix using a 600 $g{\cdot}L^{-1}$ precursor solution of $hPG_{16.5}Dea$ and a 750 $g{\cdot}L^{-1}$ precursor solution of $PEG_{6.0\ kDa}$. In the same gel matrix, the lymphoblasts show a viability of ~76% if they are encapsulated at a high cell density. For fibroblasts at a low cell density, a viability of approximately 59% is achieved by encapsulation into the same matrix, and again, the viability of these cells increases to ~89% if a high cell density is used.

We assume that the cell viability increases with the cell density due to intensified paracrine signaling:[54,55] Since the mobility of rhodamine 6G as a model molecule is reduced by the presence of the microgel matrix, we expect that other, similarly sized molecules such as growth factors, which regulate cell survival and proliferation, may also exhibit a reduced mobility as compared to that in a nongelly environment. A higher cell density may thus compensate for this reduced mobility and allow cells to chemically communicate more easily.

Doyle et al.[30] and Pishko et al.[31] obtained high cell viabilities of up to 80% upon encapsulation of fibroblasts into PEG microgels that were prepared by photoinitiated free-radical polymerization. Our approach yields even higher cell viabilities of about 90%; moreover, it prevents potential damage of labile compounds such as DNA by UV irradiation. Since the use of cross-linkable macromonomers to form the microgel matrixes allows varying many experimental parameters such as the molecular weight of the hPG and PEG building blocks, the hPG to PEG ratio, and even the type of functional groups of the building blocks, further work to investigate the influence of the physical–chemical properties of the gel matrix on other types of mammalian cells can be straightforwardly implemented.

■ CONCLUSIONS

The combination of microfluidic particle templating with bioorthogonal thiol–ene click chemistry is a powerful approach to prepare polymer microgels from synthetic macromonomers. The size, shape, and monodispersity of the microgels can be precisely controlled, and a very mild, radical-free reaction cross-links the precursor polymers. These operational features are beneficial for the encapsulation of cells. Nevertheless, we observe no clear correlation between the cell viability and microgel elasticity; instead, the interaction of several factors, including those that affect the molecular transport of metabolites and nutrients, seems to determine the cell survival ratio upon encapsulation. An advantage of the use of prefabricated macromolecular precursors for the microgel synthesis is that it allows a systematic variation of the macromonomer properties, providing more insight into the relation between the microgel properties and the viabilities of encapsulated cells. As a future perspective, further refinement of the cell-laden microgel fabrication could be achieved by combining droplet-based microfluidic methods for single cell encapsulation[56] with subsequent fluorescence-activated sorting[57] to separate microgels containing living cells from microgels containing dead cells.

■ ASSOCIATED CONTENT

Supporting Information

Full experimental details and a movie showing proliferation of yeast cells inside the microgel particles. This material is available free of charge via the Internet at http://pubs.acs.org.

■ AUTHOR INFORMATION

Corresponding Author

seiffert@chemie.fu-berlin.de

Notes

The authors declare no competing financial interest.

■ ACKNOWLEDGMENTS

We thank Florian Paulus (FU Berlin) for synthesizing hyperbranched polyclycerols. Our work at Harvard was supported by the NSF (DMR-1006546) and the Harvard MRSEC (DMR-080484); it was performed in part at the Center for Nanoscale Systems (CNS), a member of the National Nanotechnology Infrastructure Network (NNIN), which is supported by the NSF (ECS-0335765). T.R. is an Elsa–Neumann fellow of the State of Berlin and received funding from the Center for International Cooperation at FU Berlin, which is gratefully acknowledged. S.S. was a research fellow of the German National Academy of Sciences Leopoldina (BMBF-LPD 9901/8-186) and is now a Liebig fellow of the Fund of the Chemical Industry (Germany). Financial support by the Focus Area NanoScale at FU Berlin is gratefully acknowledged.

■ REFERENCES

(1) Peppas, N. A.; Hilt, J. Z.; Khademhosseini, A.; Langer, R. *Adv. Mater.* **2006**, *18*, 1345–1360.
(2) Kopeček, J. *Biomaterials* **2007**, *28*, 5185–5192.
(3) Oh, J.; Drumright, R.; Siegwart, D.; Matyjaszewski, K. *Prog. Polym. Sci.* **2008**, *33*, 448–477.
(4) Sisson, A. L.; Steinhilber, D.; Rossow, T.; Welker, P.; Licha, K.; Haag, R. *Angew. Chem., Int. Ed.* **2009**, *48*, 7540–7545.
(5) Hamidi, M.; Azadi, A.; Rafiei, P. *Adv. Drug Delivery Rev.* **2008**, *60*, 1638–1649.
(6) Richter, A.; Paschew, G.; Klatt, S.; Lienig, J.; Arndt, K.-F.; Adler, H.-J. *Sensors* **2008**, *8*, 561–581.
(7) Nguyen, M. K.; Lee, D. S. *Macromol. Biosci.* **2010**, *10*, 563–579.
(8) Drury, J. L.; Mooney, D. J. *Biomaterials* **2003**, *24*, 4337–4351.
(9) Fedorovich, N. E.; Alblas, J.; de Wijn, J. R.; Hennink, W. E.; Verbout, A. J.; Dhert, W. J. A. *Tissue Eng.* **2007**, *13*, 1905–1925.
(10) Langer, R. *Acc. Chem. Res.* **2000**, *33*, 94–101.
(11) Nicodemus, G. D.; Bryant, S. J. *Tissue Eng. Part B: Rev.* **2008**, *14*, 149–165.
(12) Khademhosseini, A.; Langer, R.; Borenstein, J.; Vacanti, J. P. *Proc. Natl. Acad. Sci. U.S.A.* **2006**, *103*, 2480–2487.
(13) Khademhosseini, A.; Langer, R. *Biomaterials* **2007**, *28*, 5087–5092.
(14) Orive, G.; Hernandez, R. M.; Gascon, A. R.; Calafiore, R.; Chang, T. M. S.; Vos, P. D.; Hortelano, G.; Hunkeler, D.; Lacik, I.; Shapiro, A. M. J.; Pedraz, J. L. *Nat. Med.* **2003**, *9*, 104–107.
(15) Chang, T. M. S. *Nat. Rev. Drug Discovery* **2005**, *4*, 221–235.
(16) Tibbitt, M. W.; Anseth, K. S. *Biotechnol. Bioeng.* **2009**, *103*, 655–663.
(17) Du, Y.; Ghodousi, M.; Lo, E.; Vidula, M. K.; Emiroglu, O.; Khademhosseini, A. *Biotechnol. Bioeng.* **2010**, *105*, 655–662.
(18) Teh, S.-Y.; Lin, R.; Hung, L.-H.; Lee, A. P. *Lab Chip* **2008**, *8*, 198.
(19) Dendukuri, D.; Doyle, P. S. *Adv. Mater.* **2009**, *21*, 4071–4086.
(20) Tumarkin, E.; Kumacheva, E. *Chem. Soc. Rev.* **2009**, *38*, 2161.
(21) Shah, R. K.; Shum, H. C.; Rowat, A. C.; Lee, D.; Agresti, J. J.; Utada, A. S.; Chu, L.-Y.; Kim, J.- W.; Fernandez-Nieves, A.; Martinez, C. J.; Weitz, D. A. *Mater. Today* **2008**, *11*, 18–27.
(22) Sugiura, S.; Oda, T.; Izumida, Y.; Aoyagi, Y.; Satake, M.; Ochiai, A.; Ohkohchi, N.; Nakajima, M. *Biomaterials* **2005**, *26*, 3327–3331.
(23) Tan, W. H.; Takeuchi, S. *Adv. Mater.* **2007**, *19*, 2696–2701.
(24) Perez-Castillejos, R. *Mater. Today* **2010**, *13*, 32–41.
(25) Jongpaiboonkit, L.; King, W. J.; Lyons, G. E.; Paguirigan, A. L.; Warrick, J. W.; Beebe, D. J.; Murphy, W. L. *Biomaterials* **2008**, *29*, 3346–3356.
(26) Chan, V.; Zorlutuna, P.; Jeong, J. H.; Kong, H.; Bashir, R. *Lab Chip* **2010**, *10*, 2062–2070.
(27) Fedorovich, N.; Oudshoorn, M.; Vangeemen, D.; Hennink, W.; Alblas, J.; Dhert, W. *Biomaterials* **2009**, *30*, 344–353.
(28) Oudshoorn, M.; Rissmann, R.; Bouwstra, J.; Hennink, W. *Biomaterials* **2006**, *27*, 5471–5479.
(29) Oudshoorn, M. H. M.; Penterman, R.; Rissmann, R.; Bouwstra, J. A.; Broer, D. J.; Hennink, W. E. *Langmuir* **2007**, *23*, 11819–11825.
(30) Panda, P.; Ali, S.; Lo, E.; Chung, B. G.; Hatton, T. A.; Khademhosseini, A.; Doyle, P. S. *Lab Chip* **2008**, *8*, 1056.
(31) Koh, W.-G.; Revzin, A.; Pishko, M. V. *Langmuir* **2002**, *18*, 2459–2462.
(32) Steinhilber, D.; Seiffert, S.; Heyman, J. A.; Paulus, F.; Weitz, D. A.; Haag, R. *Biomaterials* **2011**, *32*, 1311–1316.
(33) Bott, K.; Upton, Z.; Schrobback, K.; Ehrbar, M.; Hubbell, J. A.; Lutolf, M. P.; Rizzi, S. C. *Biomaterials* **2010**, *31*, 8454–8464.
(34) Williams, C. *Biomaterials* **2005**, *26*, 1211–1218.
(35) Li, G.-Z.; Randev, R. K.; Soeriyadi, A. H.; Rees, G.; Boyer, C.; Tong, Z.; Davis, T. P.; Becer, C. R.; Haddleton, D. M. *Polym. Chem.* **2010**, *1*, 1196.
(36) Metters, A.; Hubbell, J. *Biomacromolecules* **2005**, *6*, 290–301.
(37) Lutolf, M. P.; Tirelli, N.; Cerritelli, S.; Cavalli, L.; Hubbell, J. A. *Bioconjugate Chem.* **2001**, *12*, 1051–1056.
(38) Kade, M. J.; Burke, D. J.; Hawker, C. J. *J. Polym. Sci., Part A: Polym. Chem.* **2010**, *48*, 743–750.
(39) Elbert, D. L.; Pratt, A. B.; Lutolf, M. P.; Halstenberg, S.; Hubbell, J. A. *J. Controlled Release* **2001**, *76*, 11–25.
(40) Sletten, E. M.; Bertozzi, C. R. *Angew. Chem., Int. Ed.* **2009**, *48*, 6974–6998.
(41) Fairbanks, B. D.; Sims, E. A.; Anseth, K. S.; Bowman, C. N. *Macromolecules* **2010**, *43*, 4113–4119.
(42) Lutolf, M. P.; Raeber, G. P.; Zisch, A. H.; Tirelli, N.; Hubbell, J. A. *Adv. Mater.* **2003**, *15*, 888–892.
(43) Jin, R.; Moreira Teixeira, L. S.; Krouwels, A.; Dijkstra, P. J.; van Blitterswijk, C. A.; Karperien, M.; Feijen, J. *Acta Biomater.* **2010**, *6*, 1968–1977.
(44) Ellman, G. L. *Arch. Biochem. Biophys.* **1958**, *74*, 443–450.
(45) Zustiak, S. P.; Leach, J. B. *Biomacromolecules* **2010**, *11*, 1348–1357.
(46) McDonald, J. C.; Duffy, D. C.; Anderson, J. R.; Chiu, D. T.; Wu, H.; Schueller, O. J. A.; Whitesides, G. M. *Electrophoresis* **2000**, *21*, 27–40.
(47) Kumachev, A.; Greener, J.; Tumarkin, E.; Eiser, E.; Zandstra, P. W.; Kumacheva, E. *Biomaterials* **2011**, *32*, 1477–1483.
(48) Hiemstra, C.; van der Aa, L. J.; Zhong, Z.; Dijkstra, P. J.; Feijen, J. *Biomacromolecules* **2007**, *8*, 1548–1556.
(49) Hudalla, G. A.; Eng, T. S.; Murphy, W. L. *Biomacromolecules* **2008**, *9*, 842–849.
(50) Saxton, M. J. *Biophys. J.* **1994**, *66*, 394–401.
(51) Havlin, S.; Ben-Avraham, D. *Adv. Phys.* **1987**, *36*, 695–798.
(52) Schwille, P.; Korlach, J.; Webb, W. W. *Cytometry* **1999**, *36*, 176–182.
(53) Wachsmuth, M.; Waldeck, W.; Langowski, J. *J. Mol. Biol.* **2000**, *298*, 677–689.
(54) Lin, C.-C.; Anseth, K. S. *Proc. Natl. Acad. Sci. U.S.A.* **2011**, *108*, 6380–6385.
(55) Tumarkin, E.; Tzadu, L.; Csaszar, E.; Seo, M.; Zhang, H.; Lee, A.; Peerani, R.; Purpura, K.; Zandstra, P. W.; Kumacheva, E. *Integr. Biol.* **2011**, *3*, 653–662.
(56) Köster, S.; Angile, F. E.; Duan, H.; Agresti, J. J.; Wintner, A.; Schmitz, C.; Rowat, A. C.; Merten, C. A.; Pisignano, D.; Griffiths, A. D.; Weitz, D. A. *Lab Chip* **2008**, *8*, 1110–1115.
(57) Baret, J.-C.; Miller, O. J.; Taly, V.; Ryckelynck, M.; El-Harrak, A.; Frenz, L.; Rick, C.; Samuels, M. L.; Hutchison, J. B.; Agresti, J. J.; Link, D. R.; Weitz, D. A.; Griffiths, A. D. *Lab Chip* **2009**, *9*, 1850–1858.